

Synthesis, Characterization and Inhibition Effect of a New Schiff Base (E)-3-(((2-amino-4-methylphenyl)imino)methyl)naphthalen-2-ol on the Corrosion of Carbon Steel X48 in acidic medium

Mouzali Saida^{1,*}, Haffar Djahida¹, Bouzidi Leila¹, Bouanane Zohra²

¹ Laboratoire d'Electrochimie des Matériaux Moléculaires et des Complexes (LEMMC), Département de Génie des Procédés, Faculté de Technologie, Université Ferhat Abbas, Sétif-1, 19000, Algeria.

² Laboratoire des Matériaux Polymériques Multiphasiques (LMPMP), Département de Génie des Procédés, Faculté de Technologie, Université Ferhat Abbas, Sétif-1, 19000, Algeria.

*E-mail: mouzali2001@outlook.fr

Received: 6 April 2017 / Accepted: 11 September 2017 / Published: 12 October 2017

In the present investigation a new Schiff base named (E)-3-(((2-amino-4-methylphenyl)imino)methyl)naphthalen-2-ol (L) was synthesized, characterized, and tested as a corrosion inhibitor for Carbon steel X48 in two medium 1 M HCl and 0.5 M H₂SO₄, the corrosion efficiency coefficient was evaluated using weight loss method, Tafel polarization and electrochemical impedance spectroscopy. The experimental results suggest that this compound is an efficient corrosion inhibitor in both acidic media, and the inhibition efficiency increases with the increase of inhibitor concentration. Inhibitor adsorption on the Carbon steel X48 surface follows Langmuir isotherm. Thermodynamic parameters such as E_a , ΔH_a^0 , ΔS_a^0 , ΔH_{ads}^0 , ΔS_{ads}^0 , ΔG_{ads}^0 were obtained from Tafel polarization at different temperatures (25–55 °C). This confirms that the adsorption of the inhibitor on the surface is carried out by an intermediate adsorption between physisorption and chemisorption in both acids. The Correlation between theoretical results of the Density Functional Theory (DFT) and experimental results is discussed

Keywords: Synthesis; Schiff Base; Carbon steel; Acid solution; inhibition efficiency.

1. INTRODUCTION

There is no doubt that corrosion of metals and alloys leads to their metallic properties degradation, and makes them less effective. Consequently, the use of inhibitors is considered as one of the most practical methods for the protection against corrosion in acid media [1, 2]. In fact, inhibitors are compounds capable of controlling, reducing, or preventing when added to the medium in small

quantities the reactions between a metal and its surroundings. The most aggressive media of the metal are the acids, such as hydrochloric acid (HCl) and sulfuric acid (H₂SO₄); those last are often used as industrial surface cleaners and picklings [3].

Schiff bases are organic molecules with an azomethine bond (C=N) and are considered to be the most effective, their action mode has been the subject of many works [4-7].

Many articles cite the use of Schiff bases as effective corrosion inhibitors for steel, copper and aluminum in acidic medium [8-12]. Benabid and al. [13] investigated the inhibition effect of a new synthesized Schiff base named 1,13-bis-[(2-hydroxynaphthaldehyde) 4,7,10-trioxatridecane diimine] (HNTTD) on mild steel X48 in 1 M hydrochloric acid solution, proving that inhibition efficiency increases with increasing inhibitor concentration, they also prove from the polarization curves that the studied compound was acting as mixed type inhibitor and the adsorption of HNTTD on steel surface followed Langmuir's adsorption isotherm.

On the other hand, M.G. Hosseini and al. [14] studied the inhibitory action of three new Schiff bases viz N,N-ethylen-bis (salicylideneimine), N,N-isopropyl-bis (salicylideneimine), and N-acetylacetone imine, N-(2-hydroxybenzophenone imine) ortho-phenylen on mild steel corrosion in sulfuric acid. These Schiff bases function as good inhibitors reaching inhibition efficiencies of 97-98 % at 300 ppm concentration. The inhibitor adsorption of those three Schiff base follows Langmuir isotherm and thermodynamic calculations indicate the adsorption to be physical in nature.

The aim of this work is to study the corrosion inhibitive activity of a new synthesized Schiff base (E)-3-(((2-amino-4-methylphenyl)imino)methyl)naphthalen-2-ol on the corrosion of carbon steel X48 in two aggressive hydrochloric acid 1 M and sulfuric acid 0,5 M medium using electrochemical techniques (polarization curves and impedance spectroscopy) and by weight loss method (gravimetry), and some thermodynamic values (E_a , ΔH_a^0 , ΔS_a^0 , ΔH_{ads}^0 , ΔS_{ads}^0 , ΔG_{ads}^0) were deduced from adsorption isotherms

The Density Functional Theory method (DFT) was adopted to confirm the existence of correlation between the molecular structure of the tested compounds and its inhibitory activity.

2. EXPERIMENTAL

2.1. Materials and physical measurements

All starting materials and solvents were purchased from Merck or Aldrich and were used without further purification. Elemental Analysis System (C, H, N, S) were carried out on a "2400 Elemental Analyzer" Perkin Elmer. Melting point of the ligand was determined on a Kofler Bank 7779 apparatus. IR spectra were obtained with an FT/IR-JASCO 4200 instrument in 500-4000 cm⁻¹ range. The UV spectrum was recorded in ethanol on a U-650 JASCO spectrophotometer. ¹H NMR spectra was recorded on a Bruker Avance DPX250 spectrometer (working frequency 250 MHz) at 25 °C.

2.2. Media

The inhibitor solutions of Schiff base were prepared in 0.5 M sulfuric acid (H₂SO₄ 98 %) and 1M Hydrochloric acid (HCl 37 %). For each experiment, a freshly prepared media was used under air atmosphere without stirring. The concentration range of Schiff base inhibitor employed was varied from 10⁻⁵ M to 7.5 10⁻⁴ M, this series was determined after experimenting the inhibitor solubility in the corrosive medium.

2.3. Synthesis of Schiff base (E)-3-(((2-amino-4-methylphenyl)imino)methyl)naphthalen-2-ol (L)

Schiff base (E)-3-(((2-amino-4-methylphenyl)imino)methyl)naphthalen-2-ol (L) was synthesized according to the operating mode described in the literature [15, 16]. The reaction is conducted under stirring and refluxing. A (1 mmol, 0.122 g) diamine a 4-methyl-o-phenylenediamine in 30 ml absolute methanol solution is added, drop by drop to a 2-hydroxy naphthaldehyde (1mmol, 0.172g) in 10 ml absolute methanol solution. The mixture is refluxed and stirred for one hour while maintaining the solution temperature at 50 °C. At the end of reaction, a precipitate of orange color is obtained which, after cooling, is filtered, twice washed in methanol then dried under vacuum. The final product is recovered with: yield 80 %; M.p. 195 °C; IR (v cm⁻¹): 3397 (OH), 3318 (NH)_s - 3218 (NH)_{as}, 1648 (C=N), 1604 (C=C), 1604 (C=C); UV-Vis (Ethanol, λ_{max} nm): λ_{max} (222), λ_{max} (318), λ_{max} (443); ¹H NMR (300 MHz, MeOH, δ ppm, J Hz): 15.66 (s, 1H, OH), 9.59 (s, 1H, CH=N), 8.50 (d, J = 8.22 Hz, 1H), 7.93 (d, J = 9.08 Hz, 1H,), 7.82 (d, 8.20,1H), 7.55 (ddd, J = 8.43, 6.92, 1.39 Hz, 1H), 7.44-7.31 (m, 2H), 7.09 (d, J = 9.07 Hz, 1H), 6.67 (s, 1H), 6.54 (dd, J = 8.04, 1.27 Hz, 1H), 5.05 (s, 2H, NH₂), 2.23 (s, 3H, CH₃); Elemental analysis calculated for C₁₈H₁₆ON₂: (M = 276.35 g/mol): C, 78.26; H, 5.79; N, 10.14 %; found: C, 78.44; H, 5.45; N, 10.16 %.

2.4. Gravimetric measurement

The study of the concentration effect on the corrosion inhibitive activity of the tested compound consists in immersing carbon steel X48 samples of 9.106 cm² surface in acid in absence and presence of various inhibitor concentrations. The inhibition efficiency is determined after six hours immersion at 25 °C.

Gravimetric tests have been carried out in a 50 ml beaker. The electrolyte volume is 30 ml. Samples are immersed in oblique position, in the corrosive solution in absence and in presence of inhibitor. Before- each measure, the sample surface is polished using abrasive papers with various granulometries (from 800 to 2000), then washed with bidistilled water, degreased with acetone and dried under airflow. The sample is then weighed and immediately introduced into the electrolyte.

2.5. Electrochemical measurement

For corrosion experiments, the working electrode is a Carbon steel X48 disc-like with the

following composition: C 0.52-0.50 %, Mn 0.5-0.80 %, Si 0.40 %, P 0.035%, S \leq 0.035% and the remaining amount is Fe, of 0.19 cm² surface. At the end of each manipulation, the working electrode surface is carefully cleaned using abrasive paper with various grain sizes (800,1200 and 2000), then rinsed several times with bi-distilled water and acetone, and finally dried with Josef paper.

The electrochemical experiments were carried out on a VoltaMaster 4 software controlled Voltalab 40 and were conducted in a 200 ml volume cylindrical three-electrode cell with a double-envelope Pyrex glass cover. Reference electrode is a saturated calomel electrode (SCE), the counter-electrode is a graphite bar and the working electrode is a 0.19 cm² active surface disc-like steel.

Polarization curves are drawn in a potential range from -700 to -300 mV/SCE, with a 0.5 mV/s scan step at various temperatures between 25 °C and 55 °C.

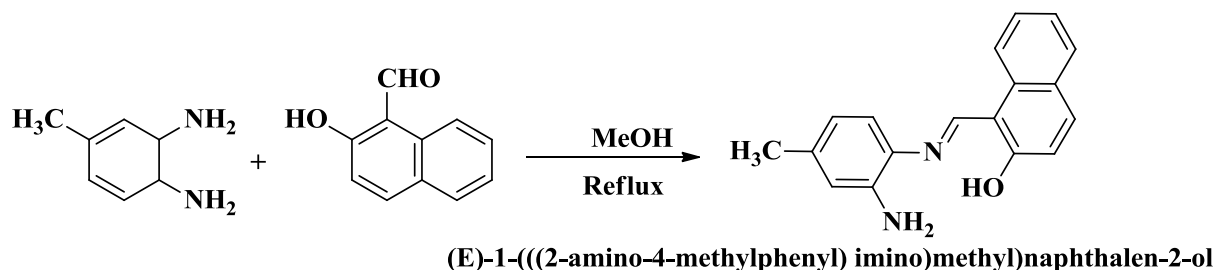
Electrochemical impedance measurements are realized after 30 minutes immersion of the material into the acidic medium by analyzing the frequency response of the electrochemical system in the range of 100 kHz to 0.1 Hz at 10 mV amplitude with 5 points by decade.

2.6. Quantum chemical calculations

The geometrically optimization of the studied Schiff base was done by Gaussian09 [17] software, using the density functional theory (DFT) with the B3LYP/6-31G (d,p) level. The energy of the highest occupied molecular orbital (E_{HOMO}), the energy of the lowest unoccupied molecular orbital (E_{LUMO}), $\Delta E = E_{LUMO} - E_{HOMO}$, the dipolar moment (μ) and the fraction of electrons transferred (ΔN) were used to analyze the inhibition capability.

3. RESULTS AND DISCUSSION

The Schiff base ligand L synthesis, named (E)-3-(((2-amino-4-methylphenyl)imino)methyl)naphthalen-2-ol consists in making contact between an aromatic diamine a 4-methyl-o-phenylenediamine, and a 2-hydroxy naphthaldehyde in heated methanol (Scheme 1).



Scheme 1. Reaction scheme for the synthesis of ligand L

3.1. Structural confirmation of the investigated compound

3.1.1. FT-IR spectra

the FT-IR spectra of this ligand indicated the formation of the Schiff base product by the absence of the carbonyl group (1700 cm^{-1}) band and the appearance of a new band at 1648 cm^{-1} , assignable to the $\nu(\text{C}=\text{N})_{\text{imine}}$ group [18]. There are other informative peaks to be expected in the region $3397\text{-}3218\text{ cm}^{-1}$ attributed to the stretching vibration of hydrogen bonded of OH group and the N-H stretching band. Absorption bands attributed to imine $\nu(\text{C}=\text{N})$ and phenolic $\nu(\text{C}-\text{O})$ groups suggested that Schiff base L exist in the solid state as OH tautomer [19].

3.1.2. $^1\text{H-NMR}$ spectra and elemental analysis

The $^1\text{H-NMR}$ spectra in methanol showed a singlet peak at 9.59 ppm which can be attributed to the imine proton ($\text{HC}=\text{N}$) [20]. In addition, two singlets peaks at around 5.0 ppm and 2.13 ppm have also been observed which can be attributed to the amine (NH_2) and methyl (CH_3) groups respectively [21]. All the other aromatic protons were observed in the expected regions [19, 22].

Elemental analysis as well as spectroscopic data of this compound is in full agreement with the formulated structure.

3.2. Weight loss measurement (Gravimetric study)

Weight loss measures are a preliminary approach to study the metal corrosion inhibition in an electrolytic solution, the method advantage is its easy processing which needs no complex apparatus.

The corrosion rate (w) is determined by the following equation (1):

$$w = \frac{\Delta m}{s \cdot t} \quad (1)$$

$$\Delta m = m_1 - m_2$$

Δm : Masse loss in mg.

m_1 : initial mass before immersion in mg, m_2 : final mass after a time t of the sample immersion in the solution in mg, s exposed surface in cm^2 and t : exposition time in the solution in hour.

The inhibition efficiency η_w (%) of the studied compound is calculated using the following equation (2):

$$\eta_w = \frac{w_0 - w_i}{w_0} * 100 \quad (2)$$

w_0 and w_i represent respectively, the corrosion rate values in absence and in presence of inhibitor.

The corrosion rate w ($\text{mg} \cdot \text{cm}^{-2} \cdot \text{h}^{-1}$) and the inhibitive efficacy η_w obtained for the ligand L at various concentrations towards the carbon steel X48 corrosion in HCl 1 M and H_2SO_4 0.5 M at $25\text{ }^\circ\text{C}$ are summarized in Table 1.

Table 1. Corrosion parameters for Carbon steel X48 in aqueous solution of 1 M HCl and 0.5 m H₂SO₄ in absence and presence of different concentrations of ligand L from weight loss measurements at 25 °C for 6 h.

Acid solution	Inhibitor concentration (M)	W (mg.cm ⁻² .h ⁻²)	η _w (%)
1 M HCl	00	0.272	
	10 ⁻⁵	0.089	67.03
	5.10 ⁻⁵	0.051	81.11
	10 ⁻⁴	0.023	91.34
	5.10 ⁻⁴	0.015	94.20
	7,5 .10 ⁻⁴	0.006	97.72
0.5 M H ₂ SO ₄	00	0.265	
	10 ⁻⁵	0.121	54.31
	5.10 ⁻⁵	0.093	64.60
	10 ⁻⁴	0.071	73.20
	5.10 ⁻⁴	0.035	86.89
	7,5.10 ⁻⁴	0.020	92.42

The variation in inhibition efficiency with concentration of ligand L is shown in Fig. 1, it can be seen that η_w increases sharply with an increase in concentration, especially in 1 M HCl solution.

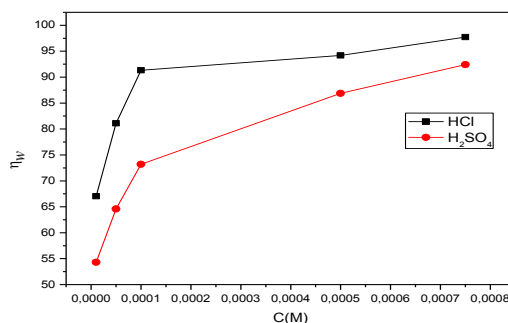


Figure 1. Plot of variation of inhibition efficiency with concentration of inhibitor L in 1 M HCl and 0.5 M H₂SO₄ at 25 °C

The inhibition efficiency η_w achieves a maximum value of 97.72 % in HCl 1M and 92.42% in H₂SO₄ 0.5 M at a concentration of 7,5.10⁻⁴ M. It is noticed, that the ligand inhibits the steel corrosion in both considered media. This behavior may be explained by a significant adsorption of the inhibitor at the carbon steel X48 surface, η_w values at any inhibitor concentration are higher in 1 M HCl solution than that in 0.5 M H₂SO₄ solution, well noticed at low concentration.

3.3. Electrochemical impedance spectroscopy (stationary method)

To confirm the results of weight loss measurement and achieve more information on the corrosion mechanism (phrase incomprehensible), electrochemical techniques were used as a more complete method (electrochemical impedance spectroscopy and polarization curves).

The electrochemical impedance spectroscopy diagrams obtained at open circuit potential, recorded after 30 minutes immersion in HCl 1 M and H₂SO₄ 0.5 M media at 25 °C with and without various concentrations of the compound L are shown in Fig. 2.

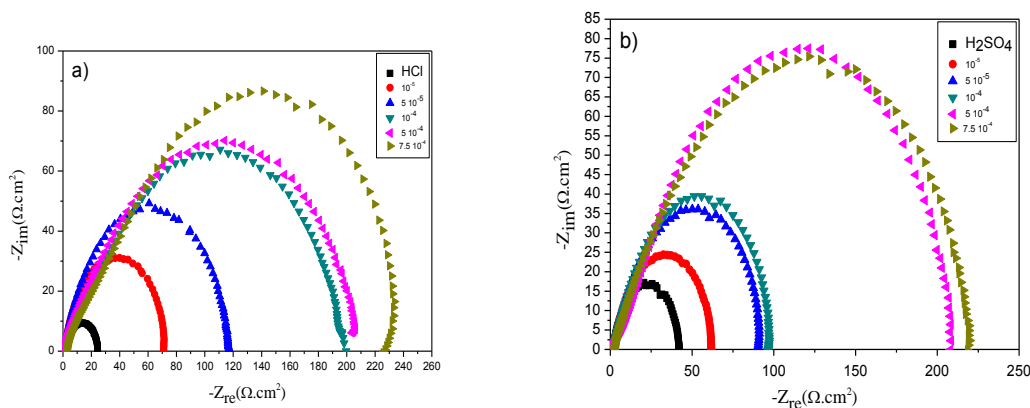


Figure 2. Nyquist plot at different concentrations of inhibitor L in 1 M HCl (a) and 0.5 M H₂SO₄ (b) solution at 25 °C

Nyquist spectrum appears as a unique capacitive loop which confirms that Carbon steel X48 corrosion in acid medium with and without inhibitor is mainly controlled by charge transfer process [23]. These diagrams have a similar shape for all concentrations, indicating there is no change during the entire corrosion mechanism. Besides, these Nyquist curves are not perfect semi-circles due to the electrode heterogeneous surface. This heterogeneity may be due to the surface roughness, impurities, inhibitor adsorption and desorption phenomena, formation of porous layers and the carbon steel chemical composition [24].

The semi-circle diameter is larger in the presence of inhibitor than that observed in the blank solution (in HCl 1M and H₂SO₄ 0.5 M medium) which increases with the increase of the concentration. This could be related to the increase in the surface coverage of steel by inhibitory molecule.

The charge transfer resistance values are calculated up on impedance difference for high and low frequencies on real axis. The corrosion inhibition efficiency of steel is calculated from the charge transfer resistance according to the equation (3):

$$\eta_z \% = \frac{Rct_i - Rct_0}{Rt_i} \times 100 \quad (3)$$

Rct₀ and Rct_i are respectively, the charge transfer resistance values of carbon steel after immersion in absence and in presence of inhibitors.

The electrochemical parameter values for various concentrations for carbon steel corrosion in

HCl 1 M and H₂SO₄ 0.5 M medium are listed in Table 2.

Table 2. Impedance parameters and inhibition efficiency values for carbon steel X48 after 30 min immersion period in 1 M HCl and 0.5 M H₂SO₄ in absence and presence of different concentrations of inhibitor L at 25 °C

Acid solution	Inhibitor concentration (M)	R_s ($\Omega \cdot \text{cm}^2$)	R_{ct} ($\Omega \cdot \text{cm}^2$)	C_{dl} ($\mu\text{F} \cdot \text{cm}^{-2}$)	η_z (%)
1 M HCl	00	1.43	23.19	433.7	
	10^{-5}	1.42	70.96	251.1	67.31
	$5 \cdot 10^{-5}$	1.38	116.2	153.3	80.04
	10^{-4}	3.31	196.5	90.66	88.19
	$5 \cdot 10^{-4}$	2.05	209.3	85.03	88.92
	$7,5 \cdot 10^{-4}$	6.2	237.4	84.44	90.23
0.5 M H ₂ SO ₄	00	1.75	40.64	493.4	
	10^{-5}	2.57	60.19	296.10	48.10
	$5 \cdot 10^{-5}$	2.44	90.14	247.10	54.91
	10^{-4}	2.83	96.13	190.66	57.72
	$5 \cdot 10^{-4}$	4.90	207.0	153.70	80.36
	$7,5 \cdot 10^{-4}$	3.71	220.2	114.10	81.54

From Table 2, it can be noticed that:

-The inhibition efficiency η_z increases with the inhibitor L concentration and achieves a maximum value of 90.23 % in HCl 1M and 81.54 % in H₂SO₄ 0.5 M at $7,5 \cdot 10^{-4}$ M. This result is in agreement with those found by gravimetric measurements.

-The charge transfer resistance (R_{ct}) increases significantly with the increasing inhibitor concentration, whereas the double-layer capacity decreases when the inhibitor is added.

-The decreasing in the double-layer capacity (C_{dl}) is due to the inhibitor adsorption at the steel surface which reduces the dielectric constant of the medium and/or increases the electric double-layer width, suggesting that the L molecule acts by adsorption at the metal/solution interface.

The same behavior is shown on the Bode-modulus plots (Fig. 3). Indeed, Inhibition effect of the inhibitor can easily be observed from the low frequency impedance modulus [25]. The low frequency impedance modulus increases with increasing the concentration of the inhibitor, which demonstrates that the adsorption of the inhibitor improves corrosion resistance of carbon steel in 1 M HCl and 0.5 M H₂SO₄ [26].

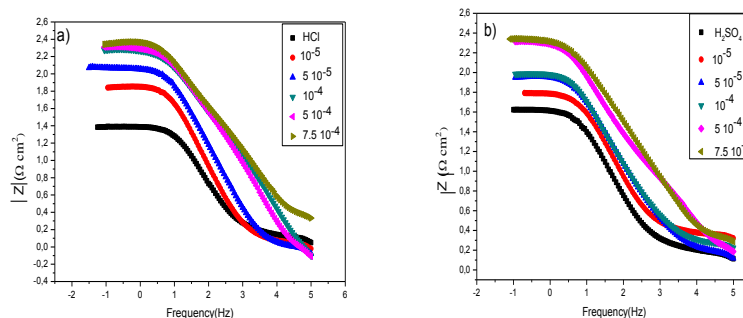


Figure 3. Bode plot at different concentrations of inhibitor L in 1 M HCl (a) and 0.5 M H₂SO₄ (b) solution at 25 °C

3.4. Polarization curves

The polarization curves in absence and in presence of ligand L, at various concentrations between 10⁻⁵ M and 7,5.10⁻⁴ M, in HCl 1M and H₂SO₄ 0.5 M of Carbon steel at 25 °C, are reported in Fig. 4. From the obtained results, it can be noticed that the addition of the compound L results systematically by a decrease of the anodic and cathodic current densities. This may be due to the adsorption of the inhibitor on the corroded surface [27].

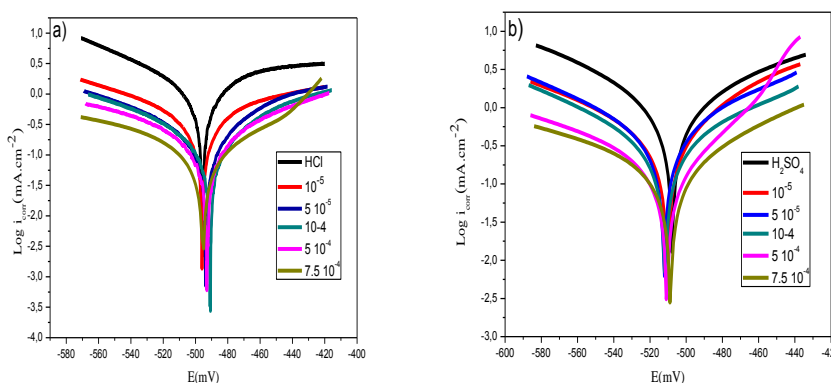


Figure 4. Tafel plot of Carbon steel X48 with different concentrations of inhibitor L in 1 M HCl (a) and 0.5 M H₂SO₄ (b) solution

The inhibition efficiency η_p obtained from the potentiodynamic polarization curves was calculated according to the following equation (4):

$$\eta_p \% = \left(\frac{i_{corr}^{\circ} - i_{corr}}{i_{corr}^{\circ}} \right) \times 100 \quad (4)$$

Where i_{corr}° and i_{corr} are the corrosion current densities values obtained by extrapolation of the linear portions of the anodic current–potential curves to the corresponding corrosion potentials (E_{corr}), during 30 minutes immersion in acid medium (HCl 1 M and H₂SO₄ 0.5 M) respectively in absence and in presence of inhibitor L.

The various ligand L corrosion parameters in both media HCl 1 M and H₂SO₄ 0.5 M obtained using this method, such as the corrosion potential E_{corr} (mV), Tafel cathodic β_c (mV/dec) and anodic β_a

(mV/dec) slope, the corrosion current density i_{corr} (mA.cm⁻²) and the inhibitive efficacy η_p (%) for various concentrations are reported in the Table 3. It is obvious that the corrosion current density values (i_{corr}) decreased from 1.15 mA.cm⁻² to 0.055 mA.cm⁻² and from 0.95 mA.cm⁻² to 0.085 mA.cm⁻² for a concentration of $7,5 \cdot 10^{-4}$ M of ligand L in HCl 1 M and H₂SO₄ 0,5 M respectively (Table 3).

Table 3. Polarization parameters and inhibition efficiency values for Carbone steel X48 after 30 minutes immersion period in 1 M HCl and 0.5 M H₂SO₄ in absence and presence of different concentrations of inhibitor L at 25 °C

Acid solution	Inhibitor concentration (M)	E_{corr} (mV/CSE)	i_{corr} (mA.cm ⁻²)	β_a (mV/dec)	β_c (mV/dec)	η_p (%)
1 M HCl	00	-495	1.15	117.4	-87.6	
	10^{-5}	-496.0	0.37	118.1	-112.3	67.82
	$5 \cdot 10^{-5}$	-493.8	0.22	79.1	-105.6	80.86
	10^{-4}	-491.2	0.11	55.2	-65.9	90.43
	$5 \cdot 10^{-4}$	-495.4	0.08	72.4	-50.3	93.04
	$7,5 \cdot 10^{-4}$	-491.1	0.05	32.6	-36.3	95.65
0.5 M H ₂ SO ₄	00	-507.8	0.95	97.5	-85.3	
	10^{-5}	-510.5	0.45	74.4	-110.8	52.63
	$5 \cdot 10^{-5}$	-512.2	0.34	70.2	-83.5	64.21
	10^{-4}	-511.7	0.26	87.4	-82.9	72.63
	$5 \cdot 10^{-4}$	-505.1	0.14	80.5	-118.9	85.26
	$7,5 \cdot 10^{-4}$	-510.7	0.08	43.0	-54.8	91.57

Polarization anodic and cathodic curves show that the addition of inhibitor L causes a decrease of anodic and cathodic current densities and modifies slightly the corrosion potential values (E_{corr}). This inhibitor may so be classified as a dual inhibitor in both media (HCl and H₂SO₄).

The inhibition efficiency η_p (%) is noticed to increase with the increasing inhibitor L concentration. This ligand protects almost totally the metal against HCl and H₂SO₄ corrosive attack. It is to be noted that the inhibitor provides a better inhibitive efficiency in HCl than in H₂SO₄. This is probably due to the significant adsorption of SO₄²⁻ ions much more voluminous than Cl⁻ ions on the active sites at the steel surface at the expense of organic molecules [28]. This result indicates clearly that adding the L inhibitor reduces the anodic dissolution of steel and slows the evolution of H⁺ proton discharge. This may result in a formation of a layer adsorbed on the metal surface.

The results obtained by gravimetric and electrochemical measurements are seen to be in agreement to each other.

To confirm our results in the both media HCl and H₂SO₄, The comparison of previous studies results with those found for similar types of Schiff base compounds, we observe that from the data

presented in Table 4, these compounds are very good Inhibitors and behave better in HCl than in H₂SO₄ [28-30]. The good activity of the inhibitor could be attributed to the presence of C = N (imine) in the molecular structure and furthermore the substitution of -OH, -NH₂ functions in its aromatic rings could increase the inhibitory performance of our Inhibitor and the three compounds reported in previous work.

Table 4. Comparison of the results obtained in this study by previous work for similar type of Schiff base compounds.

	Efficiency at optimal concentration in acidic medium η (%)			
	Present inhibitor	Wang and al [28]	Dadgarinezha and al [29]	Dadgarinezha and al [30]
Structure / Acidic solution	(E)-3-(((2-amino-4-methylphenyl) imino) methyl) naphthalen-2-ol	1, 4-bis (benzimidazolyl) benzene	N,N-O-Phenylen-bis (salicylideneimine)	Bis(2-hydroxy-1-naphthaldehyde)1,6-hexdiamine
HCl	97	97	92	97
H ₂ SO ₄	92	92	77	95

3.5. Adsorption isotherms

The inhibition of the corrosion of metals by organic compounds is reflected in their adsorption. The latter appears under three well-known aspects: physisorption, chemical adsorption or mixed adsorption (physisorption tending to chemisorption or the inverse

Metal corrosion inhibition by organic compounds is reflected in their adsorption. The latter appears under three well known aspects: physisorption, chemical adsorption or mixed adsorption (physisorption tending to chemisorption or the reverse). It depends on many factors such as the metal charge, its nature, the organic species chemical structure and the electrolyte type. It is generally accepted that the chemical adsorption process involves an electron transfer or sharing between the inhibitor molecules and the unsaturated "d" orbitals of the metal surface that allowing the formation of dative and covalent bonds, respectively.

The surface coverage values (θ) for various concentrations of the ligand in acid medium, obtained from the polarization curves, electrochemical impedance spectroscopy and gravimetric measurements at 25°C, were used to explain the best isotherm and to determine the adsorption process, it can be estimated using from the inhibitor efficiency as $\theta = \eta$ (%) / 100.

During this investigation, Langmuir, Temken and Frinmkin isotherms have been tested in order to find the most suitable isotherm. Langmuir isotherm [31] was found to be the most appropriate and can be given by the following equation (5) [32, 33]:

$$\frac{C_{inh}}{\theta} = \frac{1}{K_{ads}} + C_{inh} \quad (5)$$

Where C_{inh} the concentration of inhibitor is, K_{ads} is the adsorption equilibrium constant, and θ is the surface coverage expressed by the ration $\eta / 100$.

Fig. 5 shows that the variation of the ratio C_{inh}/θ as a function of the inhibitor concentration C_{inh} is linear for the three methods studied at 25 °C. This indicates that the ligand L adsorption on the Carbon steel surface in HCl and H_2SO_4 follows Langmuir isotherm with linear correlation coefficients ($R^2 = 0.999$) are close to 1 [34].

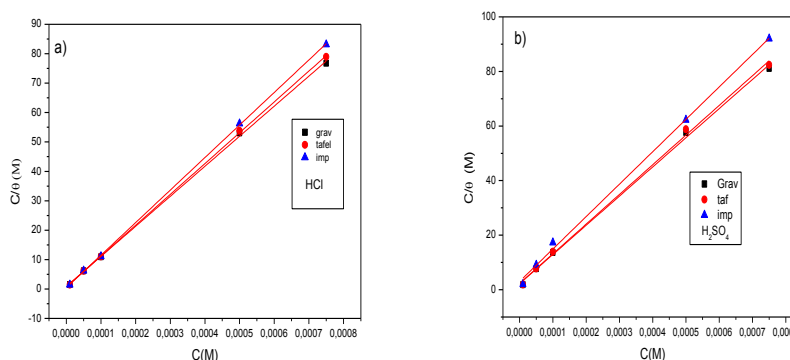


Figure 5. Langmuir adsorption of ligand on the steel surface in HCl 1M (a) and 0.5 M H_2SO_4 (b) solution using different methods.

From the intercepts of the straight lines C_{inh}/θ axis, the K_{ads} values were calculated and given in Table 5. The adsorption constant K_{ads} is related to the adsorption standard free energy (ΔG°_{ads}) by the following equation (6)[35]:

$$K_{ads} = \frac{1}{55.5} \exp\left(\frac{-\Delta G^\circ_{ads}}{RT}\right) \quad (6)$$

Where R is the gas constant ($8.314 \text{ J}\cdot\text{mol}^{-1}\cdot\text{K}^{-1}$), T the absolute temperature (K), and the value 55.5 represents the concentration of water in solution ($\text{mol}\cdot\text{l}^{-1}$) [35].

Adsorption constant values K_{ads} , and standard free energy of adsorption (ΔG°_{ads}) values calculated from Langmuir isotherms are reported in Table 5.

Table 5. Thermodynamic parameters for the adsorption of ligand in 1 M HCl and 0.5 M H_2SO_4 on the Carbon steel X48 at 25 °C

Method/ Acid	Gravimetric			Tafel			Impedance		
	R^2	$K_{ads}\cdot 10^{-4}$ (M^{-1})	ΔG°_{ads} ($KJ\cdot mol^{-1}$)	R^2	$K_{ads}\cdot 10^{-4}$ (M^{-1})	ΔG°_{ads} ($KJ\cdot mol^{-1}$)	R^2	$K_{ads}\cdot 10^{-4}$ (M^{-1})	ΔG°_{ads} ($KJ\cdot mol^{-1}$)
HCl (1 M)	0.9998	11.28	-38.80	0.9999	13.94	-39.32	0.9999	22.18	-40.47
H_2SO_4 (0.5 M)	0.9975	4.511	-36.52	0.9977	4.397	-36.46	0.9978	3.291	-35.70

Generally, ($\Delta G^{\circ}_{\text{ads}}$) values less or equal to $-20 \text{ KJ}\cdot\text{mol}^{-1}$, are related to the interactions between the charged molecules and the metal charges (physisorption), however, those close to or greater than $-40 \text{ kJ}\cdot\text{mol}^{-1}$, result in a charge transfer between the inhibitor molecules and the metal surface creating covalent or coordination bonds (chemisorption) [36 , 37].

In the present case, ΔG_{ads} values are noticed to be less than $-40 \text{ KJ}\cdot\text{mol}^{-1}$ in HCl and $-36 \text{ KJ}\cdot\text{mol}^{-1}$ in H_2SO_4 (Table 5), which indicates that the inhibitor (L) is strongly adsorbed on the steel surface as a neutral molecule via chemisorption and physisorption mechanism [38].

Furthermore, negative values $\Delta G^{\circ}_{\text{ads}}$ (from -35.70 to $-40.47 \text{ KJ}\cdot\text{mol}^{-1}$), and the high values of the adsorption constant K_{ads} are indicative of the adsorption process spontaneity and the adsorbed layer on metal surface stability [38].

3.6. Effect of the temperature

The effect of temperature on the corrosion inhibitive activity of organic compounds in acid media is very important, which can modify the behavior of inhibitors. The temperature accelerates the corrosion reactions and can weaken the corrosion steel resistance.

In the aim to study the influence of this parameter on the efficiency, a potentiodynamic analysis of steel in both media HCl and H_2SO_4 , in absence and in presence of inhibitor L, studied at concentrations from 10^{-5} to $7,5\cdot 10^{-4} \text{ M}$ and at various temperatures comprised between $25 \text{ }^{\circ}\text{C}$ and $55 \text{ }^{\circ}\text{C}$. The electrochemical properties are gathered in Table 6.

Corrosion current density evolution in the corrosive medium only (HCl, H_2SO_4) shows a rapid and regular increase, confirming an increasing metal dissolution with the increasing temperature.

The increase in the corrosion current density with the temperature in presence of inhibitor is weaker than that in the reference. These results confirm that the studied compound inhibits the corrosion process in this temperature range [25, 35, 45 and $55 \text{ }^{\circ}\text{C}$]. This result suggests that the inhibitor acts by both physical and chemical adsorption [39].

In HCl medium, the inhibition efficiency decreases from 95.21% ($25 \text{ }^{\circ}\text{C}$) to 91.51% (35°C), then becomes constant in the temperature range from $35 \text{ }^{\circ}\text{C}$ to $55 \text{ }^{\circ}\text{C}$, but in H_2SO_4 medium, it decreases within the temperature range of 25 to $45 \text{ }^{\circ}\text{C}$.

The temperature increase shifts the adsorption-desorption equilibrium in favor of the desorption process, thereby reducing the inhibitive potency of the compound (imine) [40, 41].

Many authors [42-44] use Arrhenius equation to define the temperature T effect on the corrosion current density in acid medium According to equation (7):

$$i_{\text{corr}} = A \exp\left(\frac{-E_a}{RT}\right) \quad (7)$$

Where E_a is the activation energy and A is pre-exponential factor [45].

Table 6. Effect of temperature on electrochemical parameters and inhibition efficiency for carbon steel in 1 M HCl or 0.5 M H₂SO₄ in the absence and presence of ligand L

Acid Solution		1 M HCl			0.5 M H ₂ SO ₄		
Temperature (°C)	Inhibitor C (M)	E_{corr} (mV/SCE)	i_{corr} (mA.cm ⁻²)	η_p (%)	E_{corr} (mV/SCE)	i_{corr} (mA.cm ⁻²)	η_p (%)
25	00	-495	1.15		-507.8	0.95	
	10 ⁻⁵	-496.0	0.37	67.82	-510.5	0.45	52.63
	5.10 ⁻⁵	-493.8	0.22	80.86	-512.2	0.41	58.84
	10 ⁻⁴	-491.2	1.11	91.46	-511.7	0.32	66.31
	5.10 ⁻⁴	-495.4	0.08	93.91	-505.1	0.14	81.31
	7,5 .10 ⁻⁴	-491.1	0.05	95.21	-510.7	0.08	91.05
	35	00	-514.3	1.65		-511.9	1.12
10 ⁻⁵		-506.5	0.57	65.45	-512.1	0.67	44.67
5.10 ⁻⁵		-511.8	0.35	78.78	-529.3	0.53	52.67
10 ⁻⁴		-504.6	0.26	84.24	-510.8	0.42	62.50
5.10 ⁻⁴		-536.1	0.20	87.87	-527.6	0.28	77.04
7,5.10 ⁻⁴		-534.1	0.14	91.51	-521.3	0.13	89.34
45		00	-523.8	2.399		-517.5	1.78
	10 ⁻⁵	-512.4	0.83	65.27	-514.1	1.05	41.01
	5.10 ⁻⁵	-550.1	0.51	78.66	-516.0	0.84	52.80
	10 ⁻⁴	-521.2	0.38	84.10	-518.2	0.67	62.35
	5.10 ⁻⁴	-534.4	0.29	87.86	-513.8	0.41	76.96
	7,5 .10 ⁻⁴	-534.5	0.21	91.21	-533.0	0.27	87.64
	55	00	-510.6	3.35		-517.3	3.18
10 ⁻⁵		-495.5	1.15	65.67	-517.5	1.86	41.50
5.10 ⁻⁵		-508.8	0.73	78.20	-518.6	1.55	51.25
10 ⁻⁴		-524.8	0.52	84.47	-526.8	1.22	61.63
5.10 ⁻⁴		-548.8	0.41	87.76	-535.4	0.76	76.10
7,5.10 ⁻⁴		-550.9	0.29	91.34	-542.7	0.39	87.73

The activation energies shown in Table 6 were determined by linear regression between $\ln i_{corr}$ and $1/T$ (Fig. 6) from the Arrhenius equation for various inhibitor L concentrations in two media (HCl and H₂SO₄). It is obvious that in presence of inhibitor, the activation energy values E_a are higher than those calculated with its absence in both media. This behavior is reported as being specific of a physisorption phenomenon of the inhibitor at the metal surface [46-49]. Adding the inhibitor L with increasing concentration in the two solution media HCl and H₂SO₄ increases the activation energy. This increase may be assigned to a significant decrease of the inhibitor adsorption on the steel surface

with the increasing temperature [50]. This phenomenon may be assigned by the fact that the steel corrosion process in presence of inhibitor depends not only on the reaction occurring at the bare metal surface, but also on Fe²⁺ ion diffusion through the adsorbed inhibitor layer.

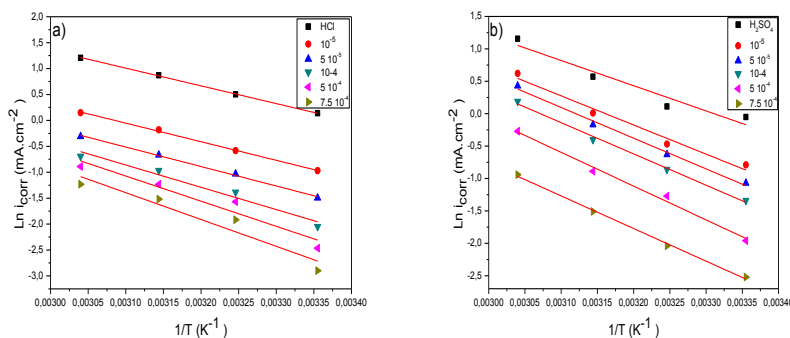


Figure 6. Arrhenius plot for Carbon steel X48 corrosion in the absence and presence of different concentrations of ligand L in 1 M HCl (a) and 0.5 M H₂SO₄ (b)

An alternative formula of Arrhenius’ equation allows determine the activation enthalpy ΔH^o_a and entropy ΔS^o_a according to the following equation [51]:

$$I_{corr} = \frac{RT}{Nh} \exp\left(\frac{\Delta S_a^o}{R}\right) \exp\left(-\frac{\Delta H_a^o}{RT}\right) \quad (8)$$

h: Planck constant, N: Avogadro’s number.

The variation of Ln (i_{corr} /T) as a function of the inverse of the temperature is a straight line (Fig. 7), with a slope equal to (ΔH^o_a/R) and an intercept (Ln R/Nh + ΔS^o_a/R) [51]. Thus, the values of ΔH^o_a and ΔS^o_a can be calculated.

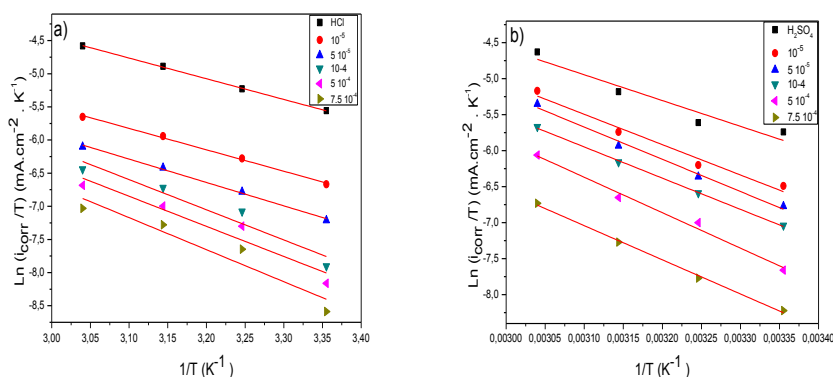


Figure 7. Transition state plot for Carbon steel corrosion in the absence and presence of different concentrations of ligand L in 1 M HCl (a) and 0.5 M H₂SO₄ (b)

The enthalpy ΔH^o_a and entropy ΔS^o_a values are given in Table 7. Positive signs of the enthalpies ΔH^o_a reflect the endothermic aspect of the steel dissolution process. In fact, the activation enthalpy ΔH^o_a increases with the concentration corresponds to a decrease in the metal dissolution [52]. This result shows that the activation energy values (E_a) are higher than their analogues of ΔH^o_a indicating that the corrosion process involves a gas reaction, forming H₂. High negative values of the

entropy ΔS_a° prove a decrease in disorder during the transformation of reactive into activated Fe-molecule complex in the solution [53].

Table 7. Activation parameters of the dissolution of carbon steel in 1 M HCl and 0.5 M H₂SO₄ in the absence and presence of different concentrations of ligand L

Acid solution	Inhibitor concentration (M)	E_a (KJ.mol ⁻¹)	ΔH_a° (KJ.mol ⁻¹)	ΔS_a° (KJ.mol ⁻¹)
1 M HCl	00	28.44	25.98	-156.43
	10 ⁻⁵	29.81	26.87	-162.42
	5 x 10 ⁻⁵	31.29	29.33	-158.65
	10 ⁻⁴	35.69	37.86	-134.78
	5 x 10 ⁻⁴	40.35	37.78	-137.10
	7.5 x 10 ⁻⁴	43.39	40.18	-132.34
	0.5 M H ₂ SO ₄	00	32.66	30.09
10 ⁻⁵		37.67	35.35	-133.39
5 x 10 ⁻⁵		39.64	37.48	-128.27
10 ⁻⁴		40.36	36.29	-134.26
5 x 10 ⁻⁴		43.49	41.10	-122.88
7.5 x 10 ⁻⁴		42.14	39.70	-132.65

3.7. Adsorption isotherms at various temperatures

Table 8. Thermodynamic parameters for the adsorption of ligand L in 1 M HCl and 0.5 M H₂SO₄ on the Carbon steel at 25–55 °C

Acid solution	T (°C)	R ²	$K_{ads} \cdot 10^{-5}$ (M ⁻¹)	ΔG_{ads}° (KJ.mol ⁻¹)	ΔH_{ads}° (KJ.mol ⁻¹)	ΔS_{ads}° (KJ.mol ⁻¹ .K ⁻¹)
1 M HCl	25	0.99992	1.394	-39.32	-4.84	115.1
	35	0.99922	1.132	-40.11		
	45	0.99876	1.072	-41.28		
	55	0.99938	1.155	-42.77		
0.5 M H ₂ SO ₄	25	0.99768	4.397	-36.46	-13.00	77.4
	35	0.99562	2.563	-36.30		
	45	0.99628	2.643	-37.56		
	55	0.99624	2.530	-38.62		

In order to compare the standard free energy of adsorption values (ΔG°_{ads}) at various temperatures from 25 to 55 °C for various inhibitor concentrations from the polarization curves, we have drawn (C/θ) as a function of inhibitor concentration (C) in HCl and H₂SO₄. The (C/θ) curve as a function of C is linear, indicating that adsorption of L follows Langmuir's isotherm model with a correlation unity [54]. Thermodynamic parameters K_{ads} and ΔG°_{ads} obtained from adsorption isotherms in the same previous conditions are listed in Table 8.

According to result shown in table 8, it is noticed that:

-The negative values of ΔG_{ads} indicate the adsorption process spontaneity and the adsorbed layer on metal surface stability [55].

-Absolute values of ΔG°_{ads} calculated (table) in H₂SO₄ are higher than 20 KJ.mol⁻¹ and lower than 40 KJ.mol⁻¹, this shows that the inhibitor was physically and chemically adsorbed. Whereas, in HCl, ΔG°_{ads} values are close or higher than 40 KJ.mol⁻¹, showing that this inhibitor was chemisorbed on the metal surface with the increasing temperature [56].

If ΔG°_{ads} values decrease as a function of temperature (become more negative), then, adsorption process is endothermic, the inhibitor adsorption is privileged by the temperature increase [57]. The calculated values of ΔG°_{ads} show that the inhibitor adsorption is a chemical endothermic process with the temperature increase. However, the physisorption phenomenon cannot be excluded. This conclusion is supported by the fact that the corrosion inhibitive activity of this ligand L decreases at high temperature.

These results confirm that the inhibitor into HCl medium contributes to a chemical adsorption stronger than in H₂SO₄. The inhibitor L adsorption may also occurred through (π) electron interactions between the molecule imine structure and the metal surface because of the existence of a much more sites on the metal surface into HCl solution because of the weak adsorption of chloride ions on the steel surface [58].

The variation of (ΔG°_{ads}) as a function of the temperature (Fig. 8) allows calculate the standard adsorption enthalpy (ΔH°_{ads}) and entropy (ΔS°_{ads}) using Gibbs–Helmholtz's equation (9) [59, 60]:

$$\Delta G^{\circ}_{ads} = \Delta H^{\circ}_{ads} - T\Delta S^{\circ}_{ads} \quad (9)$$

An adsorption endothermic process ($\Delta H^{\circ}_{ads} > 0$) is attributed to the chemisorption, however, an exothermic one ($\Delta H^{\circ}_{ads} < 0$) may be indicative of physisorption and/or chemisorption [61-63].

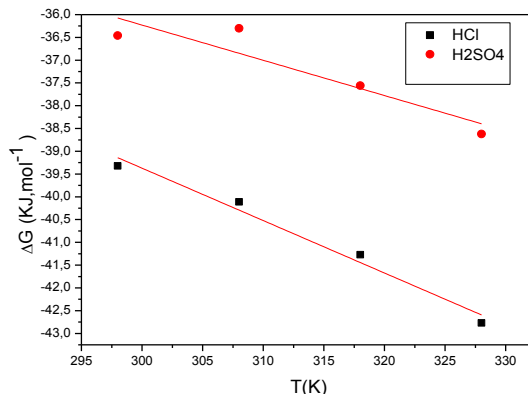


Figure 8. Variation of the standard adsorption free energy (ΔG°_{ads}) as a function of the temperature

In the present case, $\Delta H_{\text{ads}}^{\circ}$ values are negative and equal to -4.84 and -13 KJmol^{-1} in HCl and H_2SO_4 respectively, indicating that this inhibitor is physisorbed and chemisorbed on the metal surface. The standard entropy positive values $\Delta S_{\text{ads}}^{\circ}$ in presence of inhibitor mean an increase of disorder during the formation of the metal/adsorbed molecules complex [64]. Such a disorder results from desorption of several water molecules at the metal surface by a single inhibitor molecule adsorption [65-67].

Finally, it can be concluded that both adsorption modes may be considered namely, the physical adsorption and the chemisorption [68].

3.8. Quantum Chemical Studies

Quantum chemical calculations were performed in order to analyze the effect of the Schiff base molecular structure and also electronic parameters on inhibition performance of compound L.

Protection efficiency of inhibitors depends on the electronic properties of the corrosion inhibitors such as: highest occupied molecular orbital (HOMO), the lowest unoccupied molecular orbital (LUMO) [69]. In addition, Fig. 9 illustrates the optimized molecular structures and highest occupied molecular orbital of the compound L.

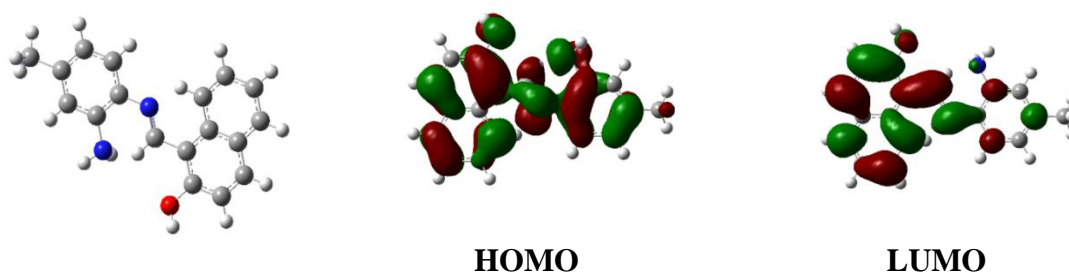


Figure 9. The optimized structure (left) and HOMO (center) and LUMO (right) distribution for molecules.

The calculated quantum chemical data reported in Table 9 include the energy of the highest occupied molecular orbital (E_{HOMO}), the energy of the lowest unoccupied molecular orbital (E_{LUMO}), the energy gap ($\Delta E = E_{\text{LUMO}} - E_{\text{HOMO}}$), the dipolar moment (μ), the absolute electronegativity (χ), global hardness (γ) and the fraction of the transferred electrons (ΔN).

Table 9. Calculated quantum chemical parameters of the Inhibitor L

Quantum chemical parameters	E_{HOMO} (eV)	E_{LUMO} (eV)	ΔE (eV)	μ (Debye)	χ (eV)	γ (eV)	ΔN
Inhibitor L	-5.16	-1.39	3.76	3.34	3.27	1.88	0.99

High value of E_{HOMO} (-5.16 eV) indicates the tendency of a molecule to donate electrons to an appropriate acceptor molecule with empty molecular orbitals.

Therefore, the energy of E_{LUMO} (-1.39) indicates the ability of a molecule to accept electrons [70, 71].

These energies of a molecule facilitate adsorption and therefore enhance the inhibition efficiency by influencing the transport process through the adsorbed layer.

In the same way, values of energy gap ($\Delta E = E_{\text{LUMO}} - E_{\text{HOMO}}$) is the measure of excitation energy to remove an electron from the last occupied molecular orbital. Low values of $\Delta E = E_{\text{LUMO}} - E_{\text{HOMO}}$ will provide good inhibition efficiencies [72].

The dipolar moment is the measure of polarity of a polar covalent bond. It is clear that, the dipolar moment of ligand L μ_L (3.34D) is more than that of $\mu_{\text{H}_2\text{O}}$ (1.88 D), this is related to stronger dipole-dipole interactions of molecules L and metallic surface. This shows the strong adsorption of ligand L on the surface of the steel.

The energies of E_{HOMO} and E_{LUMO} are related to the ionization potential (I) and the electron affinity (A) of the iron atoms and the inhibitor molecules [73], defined as $I = -E_{\text{HOMO}}$ and $A = -E_{\text{LUMO}}$. The absolute electronegativity (χ) and the global hardness (γ) of the inhibitor molecule are approximated by Eqs. (11) and (12):

$$\chi = \frac{I+A}{2} \quad (11)$$

$$\gamma = \frac{I-A}{2} \quad (12)$$

Thus, the fraction of electrons transferred from the inhibitor to metallic surface (ΔN) is calculated by equation (13) [74]:

$$\Delta N = \frac{\chi_{\text{Fe}} - \chi_{\text{inh}}}{2(\gamma_{\text{Fe}} + \gamma_{\text{inh}})} \quad (13)$$

Where the χ_{Fe} and γ_{Fe} are the absolute electronegativity and global hardness of the Fe atom, and the χ_{inh} and γ_{inh} are the absolute electronegativity and global hardness of the self-assembled molecules. The theoretical values of χ_{Fe} and γ_{Fe} are 7 eV and 0 eV [75].

The inhibitor tested has the value of $\Delta N < 3.6$ (Table 9) and therefore the molecules of the inhibitor are electron donors and the iron surface is an acceptor [76].

Inhibitors containing atoms with high negative charges are often considered to have the highest tendency to donate electrons to the metal surface [77]. Therefore, N and O atoms are the active center, which have the strongest ability of bonding to the metal surface. In addition, the areas containing N and O atoms are the most possible sites of bonding metal surface by donating electrons to the metal iron.

Finally, it is worth noting that, the data obtained from quantum chemical calculations give good evidence on the obtained results by electrochemical techniques and the adsorption of the inhibitor was mainly concentrated around the nitrogen and oxygen atoms.

4. CONCLUSION

From the above results and discussion, the following conclusions are drawn:

- The new Schiff base named (E)-3-(((2-amino-4-methylphenyl)imino)methyl)naphthalen-2-ol (L) was synthesized then purified. The chemical structure of this compound was confirmed by elemental analysis and spectroscopic methods.

- This synthesized inhibitor L was found to be effective as a corrosion inhibitor for Carbon steel in both 1M HCl and 0.5M H₂SO₄ media by weight loss and electrochemical techniques.

- The inhibition efficiencies of ligand L for Carbon steel tend to increase with increasing ligand L concentration in both acidic media. The inhibition performance in 1 M HCl solution is higher than that in 0.5 M H₂SO₄ solution at any inhibitor concentration.

- Inhibition efficiencies obtained from weight loss are in good agreement with both potentiodynamic polarization curves and electrochemical impedance spectroscopy methods.

- The polarization measurements show that the inhibitor L is found to behave as a mixed type inhibitor.

- The adsorption of this ligand L was successfully described by the Langmuir adsorption isotherm and the corresponding values of ΔG_{ads}° revealed that the adsorption mechanism of this inhibitor on Carbon steel X48 surface in 1 M HCl and 0.5 M H₂SO₄ solution is mainly due to mixed form physical and chemical adsorption.

- The study of the temperature effect on the inhibition efficiency shows that the inhibition decreases with the increasing temperature, which confirms that the adsorption of the inhibitor to the surface occurs by means of an intermediate adsorption between physisorption and chemisorption.

- Finally, this study shows a good correlation between the theoretical and electrochemical data which confirms the reliability of quantum chemical methods to investigate the corrosion inhibition of metal surfaces.

References

1. G. Trabanelli, *Corrosion.*, 47 (1991) 410.
2. K.C. Emregül, R. Kurtaran, and O. Atakol, *Corros. Sci.*, 45 (2003) 2803.
3. M.J. Banera, J. A. Caram, C.A. Gervasi, and M.V. Mirifico, *J. Appl. Electrochem.*, 44 (2014) 1337.
4. H. DeryaLeçe, K.C. Emregül, and O. Atakol, *Corros. Sci.*, 50 (2008) 1460.
5. M.G. Hosseini, M. Ehteshamzadeh, and T. Shahrabi, *Electrochimica. Acta.*, 52 (2007) 3680.
6. H. Keleş, M. Keleş, I. Dehri, and O. Serindağ, *Mater. Chemi. Phys.*, 112 (2008) 173.
7. M. Ehteshamzadeh, A.H. Jafari, E. Naderi, and M.G. Hosseini, *J. Chem. Phys.*, 113 (2009) 986.
8. M.N. Desai, M.B. Desai, C.B. Shah, and S.M. Desai, *Corros. Sci.*, 26 (1986) 827.
9. M. Ehteshamzadeh, T. Shahrabi, and M.G. Hosseini, *Appl. Surf. Sci.*, 252 (2006) 2949.
10. U.J. Naik, V.A. Panchal, A.S. Patel, and N.K. Shah, *J. Mater. Environ., Sci.* 3 (2012) 935.
11. S.S. Abd El Rehim, H.H. Hassan, and M.A. Amin, *Corros. Sci.*, 46 (2004) 5.
12. K.C. Emregül, O. Atakol, *J. Mater. Chem. Phys.*, 83 (2004) 373.
13. S. Benabid, T. Douadi, S. Issaadi, C. Penverne, and S. Chafaa, *Measurement.*, 99 (2017) 53.
14. M.G. Hosseini, M. Ehteshamzadeh, and T. Shahrabi, *Electrochimica. Acta.*, 52 (2007) 3680-3685

15. M. Hosseini, S.F.L. Mertens, M. Ghorbani, and M.R. Arshadi, *J. Mater. Chem. Phys.*, 78 (2003) 800.
16. D.K. Dey, M.K. Saha, M.K. Das, N. Bhartiya, R.K. Bansal, G. Rosair, and S. Mitra, *Polyhedron.*, 18 (1999) 2687.
17. D. Majumdar, *Int. J. Chem. Stud.*, 4 (2016) 30.
18. P. Crews, J. Rodriguez, and M. Jaspars, organic structure analysis, Oxford University Press Inc, New York, 1998.
19. J. Matijević-Sosa, M. Vinković, and D. Vikić-Topić, *Croatica. Chemica. Acta.*, 79 (2006) 489.
20. R.M. Silverstein, F.X. Webster, and D.J. Kiemle, Spectrometric identification of organic compounds, seventh ed., John Wiley & Sons, Inc., New York, 2005.
21. T.A. Alsalim, J.S. Hadi, O.N. Ali, H.S. Abbo, and S.J.J. Titinchi, *J. Chem. Cent.*, 7 (2013) 3.
22. T.K. Venkatachalam, G.K. Pierens, M.R. Campitelli, and D.C. Reutensa, *Magn. Reson. Chem.*, 48 (2010) 585.
23. R. Solmaz, *Corros. Sci.*, 52 (2010) 3321.
24. I.D. Raistrick, D.R. Franceschetti, and J.R. Macdonald, Impedance spectroscopy, in: E. Barsoukov, J.R. Macdonald (Eds.), Theory, Experimental and Applications, second ed., John Wiley & Sons, New Jersey, 2005
25. Y. Tang, F. Zhang, S. Huc, Z. Cao, Z. Wua, and W. Jing, *Corros. Sci.*, 74 (2013) 271.
26. M. Mahdavian, S. Ashhari, *Electrochim. Acta.*, 55 (2010) 1720.
27. X. Li, S. Deng, G. Muc, H. Fu, and F. Yang, *Corros. Sci.*, 50 (2008) 420.
28. X. Wang, Y. Wan, Q. Wang, and Y. Ma, *Int. J. Electrochem. Sci.*, 8 (2013) 806.
29. A. Dadgarinezhad, F. Baghaei, *GU. J. Sci.*, 3 (2012) 593.
30. A. Dadgarinezhad, I. Sheikhshoae. And F. Baghaei, *Asi. J. Chem.*, 16 (2004) 1109.
31. H.M. Abd El-Lateef, V.M. Abbasov, L.I. Aliyeva, I.T. Ismayilov, E.E. Qasimov, and M.M. Narmin, *J. Korean Chem. Soc.*, 57 (2013) 25.
32. H.J. Guadalupe, E. García-Ochoa, P.J. Maldonado-Rivas, J. Cruz, and T. Pandiyan, *J. Electroanal. Chem.*, 655 (2011) 164.
33. A.O. Yüce, B.D. Mert, G. Kardas, and B. Yazıcı, *Corros. Sci.*, 83 (2014) 310.
34. B. Liu, H. Xi, Z. Li, and Q. Xia, *Appl. Surf. Sci.*, 258 (2012) 6679.
35. L. Wang, X. Yin, W. Wang, L. Jin, and Z. Li, *Int. J. Electrochem. Sci.*, 9 (2014) 6088
36. E. Khamis, F. Bellucci, R.M. Latanision, and E.S.H. El-Ashry, *Corros. Sci.*, 47 (1991) 677.
37. F. Donahue, K. Nobe, *J. Electrochem. Soc.*, 112 (1965) 886.
38. W. Durnie, R.D. Marco, A. Jefferson, and B. Kinsella, *J. Electrochem. Soc.*, 146 (1999) 1751.
39. L. Vracar, D. Drazic, *Corros. Sci.*, 44 (2002) 1669.
40. N.M. Guan, L. Xueming, and L. Fei, *Mater. Chem. Phys.*, 86 (2004) 59.
41. I.B.Obot, N.O. Obi-Egbedi, *Corros. Sci.*, 52 (2010) 198.
42. A.E. Stoyanova, E.I. Sokolova, and S.N. Raicheva, *Corros. Sci.*, 39 (1997) 1595.
43. A.S. Fouda, S.S Elkaabi, and A.K. Mohamed, *Anti-Corros. Methods. Mater.*, 36 (1989) 9.
44. E. Stupnisek-Usac, Z. Ademovic, Proceedings of the 8th European Symposium on Corrosion Inhibitors, Ann. Univ. Ferrara (Italy), N. S. Sez suppl. 3, 1995, V 1, p. 257.
45. M.J. Bahramia, S.M.A. Hosseinia, and P. Pilvarb, *Corros. Sci.*, 52 (2010) 2793
46. R.L. Liu, Y.J. Qiao, M.F. Yan, and Y.D. Fu, *J. Mater. Sci. Technol.*, 28 (2012) 1046.
47. Z. Tianpei, M. Guannan, *Corros. Sci.*, 41 (1999) 1937.
48. H. Jafari, I. Danaee, H. Eskandari, and M. Rashvand Avec, *J. Mater. Sci. Technol.*, 30 (2014) 239.
49. W. Durnie, R.D. Marco, A. Jefferson, and B. Kinsella, *J. Electrochem. Soc.*, 146 (1999) 1751.
50. K.M. Hijazi, A.M. Abdel-Gaber, and G.O. Younes, *Int. J. Electrochem. Sci.*, 10 (2015) 4366
51. E.A. Noor, *Int. J. Electrochem. Sci.*, 2 (2007) 996.
52. M. Dahmani, A. Et-Touhami, S.S. Al-Deyab, B. Hammouti, and A. Bouyanzer, *Int. J. Electrochem. Sci.*, 5 (2010) 1060.

53. S.K.A. Ali, M.T. Saeed, and S.U. Rahman, *Corros. Sci.*, 45 (2003) 253.
54. Y. Xie, Y. Liu, and Z. Yang, *Int. J. Electrochem. Sci.*, 10 (2015)1292
55. Y. Zhou, S. Zhang, L. Guo, S. Xu, H. Lu and F. Gao, *Int. J. Electrochem. Sci.*, 10 (2015) 2072
56. A. S. El-Tabei, M.A. Hegazy, A.H. Bedair, and M.A. Sadeq, *J. Surfact. Deterg.*, 17 (2014) 341.
57. L. Tang, G. Mu, and G. Liu, *Corros. Sci.*, 45 (2003)2251.
58. O. Benali, L. Larabi, M. Traisnel , L. Gengenbre, and Y. Harek, *Appl. Surf. Sci.*, 253 (2007) 6130.
59. F. Bentiss, M. Lebrini, and M. Lagrenée, *Corros. Sci.*, 47 (2005) 2915.
60. E.A. Noor, A.H. Al-Moubaraki, *Mater. Chem. Phys.*, 110 (2008) 145.
61. M.A. Migahed, M.A. Hegazy, and A.M. Al-Sabagh, *Corros. Sci.*, 61 (2012) 10.
62. S.Pournazari, M.H. Moayed, and M. Rahimizadeh, *Corros. Sci.*, 71 (2013) 20.
63. X. Li, G. Mu, *Appl. Surf. Sci.*, 252 (2005) 1254.
64. L. Larabi, O. Benali, S.M. Mekelleche, and Y. Harek, *Appl. Surf. Sci.*, 253 (2006) 1371.
65. H. Ashassi-Sorkhabi, B. Shaabani, and D. Seifzadeh, *Electrochim. Acta.*, 50 (2005) 3446.
66. G. Gece, *Corros. Sci.*, 50 (2008) 2981.
67. R. Fuchs-Godec, V. Doleček, *Colloids Surf. A.*, 244 (2004) 73.
68. M. Dahmani, A. Et-Touhami, S.S. Al-Deyab, B. Hammouti, and A. Bouyanzer, *Int. J. Electrochem. Sci.*, 5 (2010) 1060.
69. M. Finsgar, A. Lesar, A. Kokalj, and I. Milosev, *Electrochim. Acta.*, 53 (2008) 8287.
70. D.K. Yadav, B. Maiti, and M.A. Quraishi, *Corros. Sci.*, 52 (2010) 3586.
71. J. Zhang, G. Qiao, S. Hu, Y. Yan, Z. Ren, and L. Yu, *Corros. Sci.*, 53 (2011) 147.
72. Z. Zhang, N.Tian, X. Li, L. Zhang , L. Wu, and Y. Huang, *Appl. Surf. Sci.*, 375 (2015) 845.
73. H. Tian, W. Li, K. Cao, and B. Hou, *Corros. Sci.*, 73 (2013) 281.
74. H. Zhao, X. Zhang, L. Ji, H. Hu, and Q. Li, *Corros. Sci.*, 83 (2014) 261.
75. K. Zhang, B. Xu, W. Yang, X. Yin, Y. Liu, and Y. Chen, *Corros. Sci.*, 90 (2015) 284.
76. A.Y. Musa, R.T.T. Jalgham, and A.B. Mohamad, *Corros. Sci.*, 56 (2012) 176.
77. H. Ju, Z.P. Kai, and Y. Li, *Corros. Sci.*, 50 (2008) 865.

© 2017 The Authors. Published by ESG (www.electrochemsci.org). This article is an open access article distributed under the terms and conditions of the Creative Commons Attribution license (<http://creativecommons.org/licenses/by/4.0/>).